Journal of Applied Sciences

ISSN 1812-5654

Journal of Applied Sciences 10 (23): 3014-3020, 2010
ISSN 1812-5654

Investigating the Performance of Shunt FACTS for the Operation of Induction Motors under Different Voltage Sag Conditions

M. Hedayati, N. Mariun, H. Hizam and S.M. Bashi
Department of Electrical and Electronic Engineering, University Putra Malaysia, Malaysia

Abstract: Shunt FACTS devices are prevalent in industrial application of induction motors. These equipments are effective to compensate disturbances and increase motor speeding up. In this study an assessment study between two different shunt FACTS (SVC and STATCOM) installed on terminals of motor is done. A conventional PI controller is used to control the thyristor firing angle of SVC or phase angle of STATCOM. A pole placement method is applied to specify the perfect gain settings of the controllers. The results of simulations display that STATCOM has better response over SVC for improving dynamic behavior of induction motor under ideal supply conditions. Power quality problem that influence the dynamic behavior of induction motor, include non ideal conditions such as harmonics, interruptions, voltage unbalance and voltage sags. Whereas voltage sags is one of the main cause of disturbances in distribution systems, the performances of the induction motor under symmetrical and unsymmetrical voltage sags are investigated in this study. The results prove that STATCOM is more effectual than SVC for reduction of transients and refinement the voltage profile.

Key words: Induction motors, SVC, STATCOM, voltage sag

INTRODUCTION

Many studies and investigations have been carried out to assess, satisfy and enhance the power quality of the electric power system (Souto *et al*., 1998). It is well known that around 80% of electrical industrial loads consist of three phase induction motors. Induction motors need a high current and reactive power at starting. Starting of a large electrical motors connected to a bus with small short circuit power, will produce disturbance for supply network and local consumers. This disturbance generally is in the form of voltage dip and will cause power quality of the network to decrease. Furthermore abatement of voltage will result in reduction of starting torque and consequently time of motor speeding up will be increased (Hedayati and Oraee, 2005). Consequently, any power quality and energy resource survey approach should take into consideration the behavior and performance of these devices under ideal and non-ideal supply conditions.

To compensate the disturbance during the starting, it is proposed to use Shunt FACTS devices such as SVC or STATCOM. These types of compensators increase the motor speeding up and improve the voltage profile. The fundamental difference in operation principle between SVC and STATCOM is that STATCOM is a converter-based var generation function as shunt-connected synchronous voltage source; whereas SVC is thyristor controlled reactors and thyristor switched capacitors, function as a shunt connected controlled reactive admittance. In addition to that, STATCOM has the ability to exchange real power from the system if it is equipped with an energy storage element at its dc terminal. Major advantages of STATCOM over the conventional SVC are significant size reduction, reduced number of passive elements due to the development of capacitor technology, ability to supply required reactive power even at low bus voltage, better control stability and lower harmonics (Song and Johns, 1999; Hingorani and Gyugyi, 2000).

Power quality that is concerned with variations of the voltage from its ideal waveform, affect the dynamic behavior of induction motors. Power quality occurrence includes the small deviations from the rated or preferred value called voltage variations and immediate deviations from its standard or ideal wave form are called events. One of the most popular events in the power system is voltage sags. Voltage sags are short period lessening of rms voltage, caused by short circuits, over loads and starting of large motor (Bollen, 2000).

In this study, comprehensive assessment of the effects of STATCOM and SVC controllers has been carried out for dynamic behaviors of induction motor

Corresponding Author: M. Hedayati, Department of Electrical and Electronic Engineering, University Putra Malaysia, Malaysia
Tel: 0060-3-89483484, 0060-132699067

starting under ideal supply conditions. Also, the performances of induction motor operations with shunt FACTS under symmetrical and unsymmetrical voltage sags are investigated.

SYSTEM MODELING

The system under study is the machine, a network and infinite bus where FACTS device (e.g., STATCOM or SVC) is installed on the terminal of the induction motors. Figure 1 shows the system modeling with a SVC which consists of fixed shunt Capacitor (FC) and Thyristor Controlled Reactor (TCR), while Fig. 2 shows with a STATCOM which consists of DC capacitor, a three phase GTO based Voltage Source Converter (VSC) and a step down transformer.

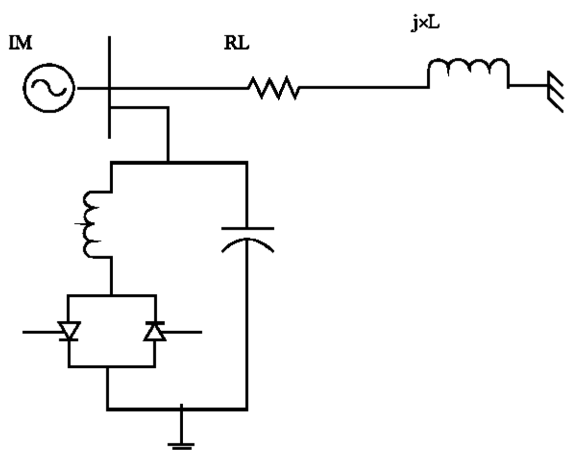

Fig. 1: System modeling with a SVC

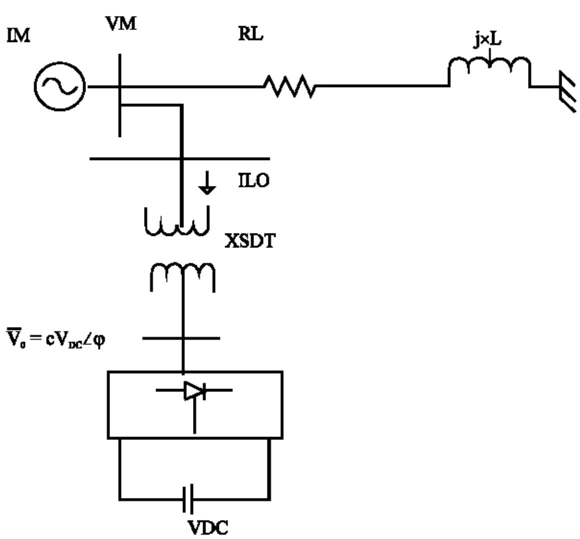

Fig. 2: System modeling with a STATCOM

Motor model: In this study, the induction motor will be presented by Park model. The complete electro mechanical equations are as follows (Hedayati and Oraee, 2005):

$$V_{qsm} = \frac{R_{sm}}{D}\left[X'_{rr}\Psi_{qsm} - X_M\Psi'_{qrm}\right] + \left(\frac{\omega_d}{\omega_b}\right)\Psi_{dsm} + \frac{\Psi^{o}_{qsm}}{\omega_b} \tag{1}$$

$$V_{dsm} = \frac{R_{sm}}{D}\left[X'_{rr}\Psi_{dsm} - X_M\Psi'_{drm}\right] + \left(\frac{\omega_d}{\omega_b}\right)\Psi_{qsm} + \frac{\Psi^{o}_{dsm}}{\omega_b}$$

$$V'_{qrm} = \frac{R'_{rm}}{D}\left[X_{ss}\Psi'_{qrm} - X_M\Psi_{qsm}\right] + \left(\frac{\omega_d - \omega_{rm}}{\omega_b}\right)\Psi'_{drm} + \frac{\Psi'^{o}_{qrm}}{\omega_b}$$

$$V'_{drm} = \frac{R'_{rm}}{D}\left[X_{ss}\Psi'_{drm} - X_M\Psi_{dsm}\right] + \left(\frac{\omega_d - \omega_{rm}}{\omega_b}\right)\Psi'_{qrm} + \frac{\Psi'^{o}_{drm}}{\omega_b}$$

$$2H_M\left(\frac{\omega_{rm}}{\omega_b}\right)^{o} = T_{em} - T_{Lm}$$

Where:

$$X_{ss} = X_{ls} + X_M,\ X'_{rr} = X'_{lr} + X_M \tag{2}$$

and

$$D = X_{ss}X'_{rr} - X^2_M$$

The expressions for the electromagnetic torque and inertia coefficient respectively are:

$$T_{em} = \frac{X_M}{D}\left(\Psi_{qsm}\Psi'_{drm} - \Psi_{dsm}\Psi'_{qrm}\right) \tag{3}$$

$$H_M = \frac{1}{2}\left(\frac{2}{P_m}\right)^2 J_m\frac{\omega_b^2}{P_B}$$

A list of symbols is given in the Appendix A.

SVC model: As mentioned, the model of SVC in this studyis FC-TCR. The dynamic equations of SVC which are presented by Park model are as follows (Hedayati and Oraee, 2005):

$$i_{Lq} = \left(\frac{-\omega_b}{\omega_d}\right)\frac{1 - C(\alpha)}{X_{in}}V_{dsm},\ i_{Ld} = \left(\frac{\omega_b}{\omega_d}\right)\frac{1 - C(\alpha)}{X_{in}}V_{qsm} \tag{4}$$

$$i_{Cq} = \frac{\omega_d}{\omega_b}\frac{V_{dsm}}{X_C},\ i_{Cd} = \frac{-\omega_d}{\omega_b}\frac{V_{qsm}}{X_C}$$

where:

$$C(\alpha) = \frac{2\alpha - \sin(2\alpha)}{\pi} - 1 \tag{5}$$

α is firing angle of thyristor.

STATCOM model: The STATCOM is modeled as a voltage-sourced converter behind a step down transformer as shown in Fig. 2. The STATCOM generates a controllable AC voltage source $V_{out}(t) = V_0 \sin(\omega t - \psi)$ behind the leakage reactance. The voltage difference between the STATCOM bus AC voltage and $V_{out}(t)$ produces active and reactive power exchange between the STATCOM and the power system (Hedayati and Oraee, 2005; Rahim and Kandlawala, 2004; Wang, 1999; Seyed *et al*., 2005).

From Fig. 2 we have:

$$\bar{I}Lo = I_{Lod} + jI_{Loq} \tag{6}$$

The DC voltage V_{DC} is governed by:

$$\frac{dV_{DC}}{dt} = \frac{I_{DC}}{C_{DC}} = \frac{c}{C_{DC}}\left(I_{Lod}\cos\varphi + I_{Loq}\sin\varphi\right) \tag{7}$$

where, C_{DC} the dc capacitor is value and I_{DC} is the capacitor current. The output voltage phasor is:

$$\bar{V}o = cV_{DC}(\cos\varphi + j\sin\varphi) = cV_{DC}\angle\varphi \tag{8}$$

For the PWM inverter; c = mk and k is the ratio between AC and DC voltage; m is the modulation ratio defined by PWM and ϕ is phase angle defined by the PWM. From Fig. 2:

$$\bar{V}M - \bar{V}0 = jX_{SDT}\bar{I}Lo \rightarrow \bar{I}Lo = \frac{\bar{V}M - \bar{V}0}{jX_{SDT}} \tag{9}$$

that:

$$\bar{V}M = V_{dsm} + jV_{qsm}$$

Substituting Eq. 6 into Eq. 9 gives:

$$\bar{I}Lo = I_{Lod} + jI_{Loq} = \frac{V_{dsm} + jV_{qsm} - cV_{DC}(\cos\varphi + j\sin\varphi)}{jX_{SDT}} \tag{10}$$

From the above, it can be shown that I_{Loq} and I_{Lod} equations are written as:

$$I_{Loq} = \left(\frac{cV_{DC}\cos\varphi - V_{dsm}}{X_{SDT}}\right) \qquad I_{Lod} = \left(\frac{V_{qsm} - cV_{DC}\sin\varphi}{X_{SDT}}\right) \tag{11}$$

Transmission line model: It is possible to model a short transmission line as a constant resistance and reactance. The dynamic model of transmission line presented by Park model is for Fig. 1 as:

$$\begin{aligned} V_{qsm} &= V_{q\infty} - R_L\left(i_{qsm} + i_{Cq} + i_{Lq}\right) - \frac{X_L}{\omega_b}\left(i_{qsm} + i_{Cq} + i_{Lq}\right)^{\circ} - X_L\left(i_{dsm} + i_{Cd} + i_{Ld}\right) \\ V_{dsm} &= V_{d\infty} - R_L\left(i_{dsm} + i_{Cd} + i_{Ld}\right) - \frac{X_L}{\omega_b}\left(i_{dsm} + i_{Cd} + i_{Ld}\right)^{\circ} + X_L\left(i_{qsm} + i_{Cq} + i_{Lq}\right) \end{aligned} \tag{12}$$

And the model can also be expressed for Fig. 2 as:

$$\begin{aligned} V_{qsm} &= V_{q\infty} - R_L\left(\left(i_{qsm} + i_{Loq}\right) - \frac{X_L}{\omega_b}\left(i_{qsm} + i_{Loq}\right)^{\circ} - X_L\left(i_{dsm} + i_{Lod}\right) \\ V_{dsm} &= V_{d\infty} - R_L\left(\left(i_{dsm} + i_{Lod}\right) - \frac{X_L}{\omega_b}\left(i_{dsm} + i_{Lod}\right)^{\circ} - X_L\left(i_{qsm} + i_{Loq}\right) \end{aligned} \tag{13}$$

The relationship between stator currents and flux linkages of quadrate and direct axes components are written as (Rahim and Baber-Abbas, 2007):

$$\begin{aligned} i_{qsm} &= \frac{X'_{rr}}{D}\Psi_{qsm} - \frac{X_M}{D}\Psi'_{qrm} \\ i_{dsm} &= \frac{X'_{rr}}{D}\Psi_{dsm} - \frac{X_M}{D}\Psi'_{drm} \end{aligned} \tag{14}$$

Linearized model: In the design of electromechanical mode damping controllers, the linearized incremental model around a nominal operation point is usually employed. Linearizing the expressions of V_{sqm} and V_{dsm} and substituting into the linear form of (1)-(11) yield the following lineraized model for SVC:

$$\begin{bmatrix} \Delta\psi_{qsm} \\ \Delta\psi_{dsm} \\ \Delta\psi'_{qrm} \\ \Delta\psi'_{drm} \\ \frac{\Delta\omega_{rm}}{\omega_b} \\ \Delta\alpha \end{bmatrix}^{\circ} = \underset{6\times6}{[A]}\begin{bmatrix} \Delta\psi_{qsm} \\ \Delta\psi_{dsm} \\ \Delta\psi'_{qrm} \\ \Delta\psi'_{drm} \\ \frac{\Delta\omega_{rm}}{\omega_b} \\ \Delta\alpha \end{bmatrix} + \underset{6\times4}{[B]}\left[\Delta U_{USVC}\right]\left[\frac{\Delta\omega_{rm}}{\omega_b}\right] = \underset{1\times6}{[C]}\begin{bmatrix} \Delta\psi_{qsm} \\ \Delta\psi_{dsm} \\ \Delta\psi'_{qrm} \\ \Delta\psi'_{drm} \\ \frac{\Delta\omega_{rm}}{\omega_b} \\ \Delta\alpha \end{bmatrix} \tag{15}$$

And for STATCOM expressed as:

$$\begin{bmatrix} \Delta\psi_{qsm} \\ \Delta\psi_{dsm} \\ \Delta\psi'_{qrm} \\ \Delta\psi'_{drm} \\ \frac{\Delta\omega_{rm}}{\omega_b} \\ \Delta\varphi \end{bmatrix}^{\circ} = \underset{6\times6}{[A]}\begin{bmatrix} \Delta\psi_{qsm} \\ \Delta\psi_{dsm} \\ \Delta\psi'_{qrm} \\ \Delta\psi'_{drm} \\ \frac{\Delta\omega_{rm}}{\omega_b} \\ \Delta\varphi \end{bmatrix} + \underset{6\times4}{[B]}\left[\Delta U_{STATCOM}\right]\left[\frac{\Delta\omega_{rm}}{\omega_b}\right] = \underset{1\times6}{[C]}\begin{bmatrix} \Delta\psi_{qsm} \\ \Delta\psi_{dsm} \\ \Delta\psi'_{qrm} \\ \Delta\psi'_{drm} \\ \frac{\Delta\omega_{rm}}{\omega_b} \\ \Delta\varphi \end{bmatrix} \tag{16}$$

In short:

$$\begin{cases} X^0 = AX + BU \\ Y = CU \end{cases} \tag{17}$$

where, A and B are constant linearization matrices and C represents the relation between state vector and the chosen output.

DESIGN OF CONTROLLER

In this study, PI controller is used to control the thyristor firing angle (α) of SVC or phase angle (ϕ) of STATCOM. α (or ϕ) adjust according to variation in terminal voltage v_t and angular speed ω. The block diagram of SVC and STATCOM controllers is shown in Fig. 3. The PI controllers are normally located in the feedback route. An extra washout block is embraced in series with the controller to remove any undesirable signal in the steady state (Rahim and Baber-Abbas, 2007). The function of controller in the feedback loop is composed as a pole placement method was used to specify perfect gain settings, K_P and K_I of the controller. The control signal from the PI can be represented by:

$$U(s) = H(s)Y(s) = \frac{sT_\omega}{1+sT_\omega}(K_P + \frac{K_I}{s})Y(s) \quad (18)$$

It is easy to see that the characteristic equation of the close loop system is:

$$1 - C(sI - A)^{-1}BH(s) = 0 \quad (19)$$

If λ is the system eigen value to be assigned, we have:

$$H(\lambda) = \frac{1}{C(\lambda I - A)^{-1}B} = H(\lambda) = \frac{\lambda T_\omega}{1+\lambda T_\omega}(K_P + \frac{K_I}{\lambda}) \quad (20)$$

Assume that the value of T_ω is given, we need to assign a pair of eigen values to obtain the values of K_P and K_I (Hedayati, 2002):

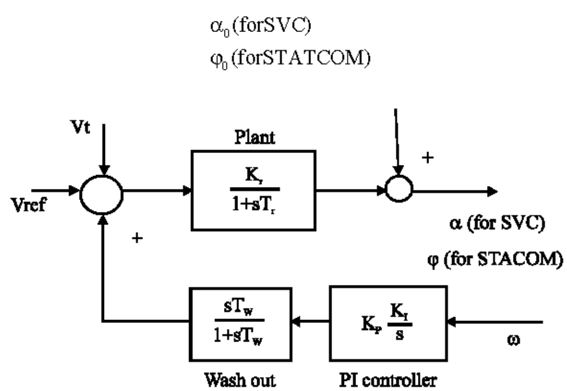

Fig. 3: PI controller configuration of SVC and STATCOM

SIMULATION RESULTS

Study of different shunt FACTS effects: The results of simulation for starting of induction motor in MATLAB programme are shown on Fig. 4 and 5. Figure 4 displays the rotor speed of the motor and Fig. 5 shows the terminal voltage of the motor for three cases: without any compensator, using SVC and using STATCOM model based on Fig. 1 and 2. The values of K_P and K_I are 50 and 0.00145, respectively. The parameters of the system are given in Appendix B. It is clear that the time of motor speeding up is lower when the STATCOM is used; besides the dip of voltage without using any compensator is almost 20%; using SVC the voltage profile is improved and declined around 10%. With utilization the STATCOM, voltage dip is decreased considerably less than 5%.

Power quality problem: Power quality context that influence the dynamic behavior of induction motor, include non ideal conditions such as harmonics, interruptions, voltage unbalance and voltage sags. Between these conditions, the voltage sags and short interruptions are very important because the voltage sags are the main cause of disturbances in distribution systems

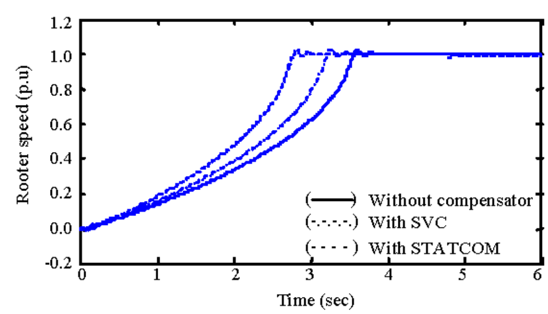

Fig. 4: Rotor speed of motor under ideal supply condition

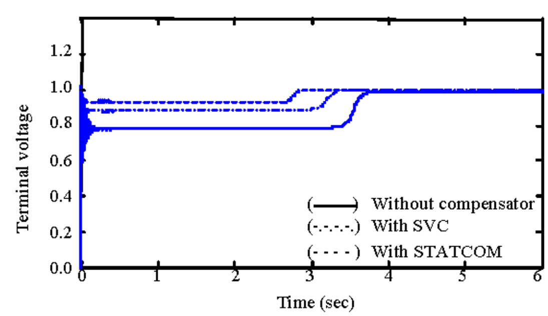

Fig. 5: Terminal voltage of motor under ideal supply condition

Table 1: Definition of symmetrical and unsymmetrical voltage sags

Symmetrical voltage sag	Unsymmetrical voltage sag
$V_a = hV$	$V_a = (\frac{2}{3}+\frac{h}{3})V$
$V_b = -\frac{1}{2}hV + j\frac{\sqrt{3}}{2}hV$	$V_b = -\frac{1}{6}(2+h)V + j\frac{\sqrt{3}}{2}hV$
$V_c = -\frac{1}{2}hV - j\frac{\sqrt{3}}{2}hV$	$V_c = -\frac{1}{6}(2+h)V - j\frac{\sqrt{3}}{2}hV$

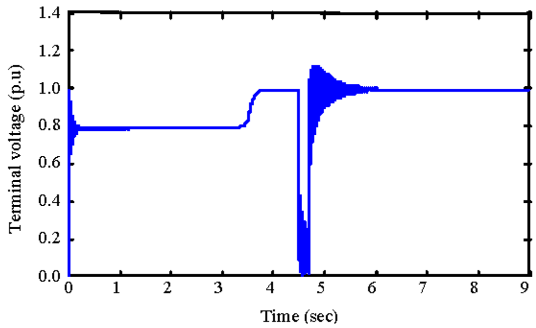

Fig. 6: Terminal voltage of motor under symmetrical voltage sag without compensator

(Gomez and Morcos, 2002). Voltage sags (or voltage dips) are unexpected reduction on the rms voltage that may lead to deficiency or crashing of responsive equipment frequently used in industrial applications (Bollen, 2000; Juarez *et al*., 2009). On the other hand, voltage sag is defined as decreasing in rms supply voltage between 0.1 and 0.9 p.u. with duration of 0.5 cycles to 1 min (Dugan *et al*., 1996).

Due to dissimilar types of faults in power systems, dissimilar types of voltage sag can be constructed. Different kinds of connection of transformers in power grid will produce different types of voltage sags. Voltage sags are divided to seven categories; but one type is symmetrical and between other types that are known unsymmetrical voltage sags, one type has the serious effect on the performance of the system (Guasch *et al*., 2004). Table 1 shows the definition of the symmetrical and unsymmetrical voltage sags.

The effects of SVC and STATCOM on dynamic performances of starting of induction motor under symmetrical voltage sag are specified on Fig. 6. The duration of voltage sag is 0.2 sec, starting at $t_{on\text{-}sag}$ = 4.5 sec and stopping at $t_{off\text{-}sag}$=4.7 sec. Sag magnitude is 90% (h = 0.1). Figure 6 shows the terminal voltage of motor without compensator, so Fig. 7 and 8 display the voltage of terminal using the SVC and STATCOM respectively. It is shown that the transient of voltage after stopping the voltage sag is lower with applying of shunt FACTS. Utilization of STATCOM is very effectual, because the transient of voltage is

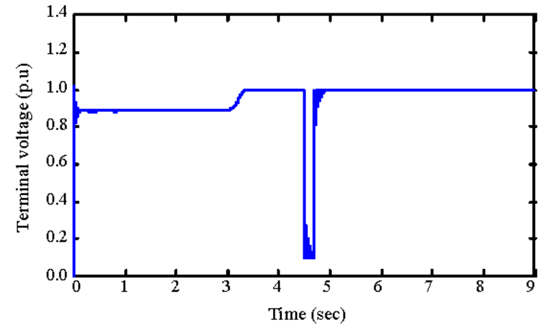

Fig. 7: Terminal voltage of motor under symmetrical voltage sag with SVC

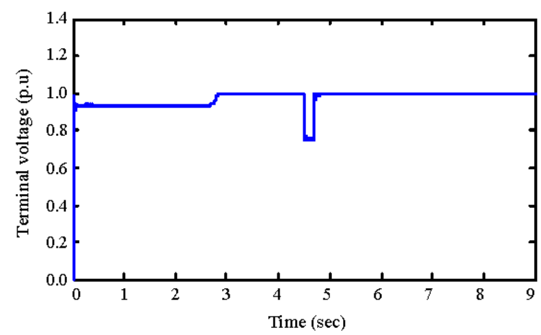

Fig. 8: Terminal voltage of motor under symmetrical voltage sag with STATCOM

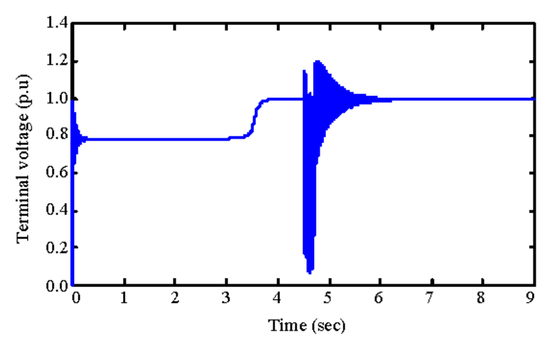

Fig. 9: Terminal voltage of motor under unsymmetrical voltage sag without compensator

remarkably receded and the profile of voltage has better dynamic performance.

Figure 9 shows the terminal voltage of motor without using any compensator. Figure 10 and 11 display the terminal voltage of motor with SVC and STATCOM when unsymmetrical voltage sag is applied. Lower voltage transients and better dynamic behavior is observed when using STATCOM over SVC.

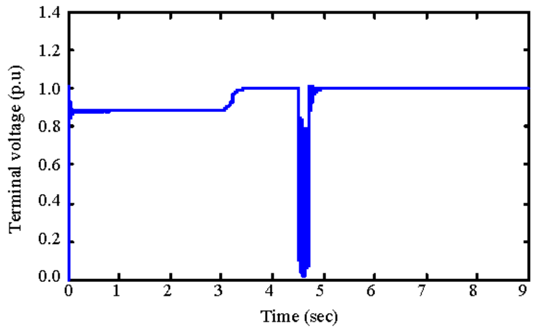

Fig. 10: Terminal voltage of motor under unsymmetrical voltage sag with SVC

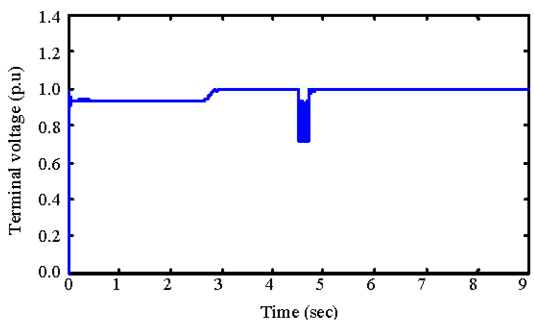

Fig. 11: Terminal voltage of motor under unsymmetrical voltage sag with STATCOM

CONCLUSION

In this study, the application o shunt FACTS installed on terminals of induction motor are presented and compared together. The results of simulations show that these devices are useful for increasing motor speeding up and getting better voltage profile. Computer test results prove this point that STATCOM is more effectual than SVC for compensation disturbances and improving dynamic behavior of large induction motor under ideal supply condition. Whereas voltage sags is one of the most conventional power quality contexts in power systems, the performances of the system under symmetrical and unsymmetrical voltage sags are investigated. The results show that utilization of STATCOM is considerably forceful and is more suitable than SVC for decreasing transients and amending the voltage profile.

APPENDIX A: NOMENCLATURE

X_L = Transmission line reactance
R_L = Transmission line resistance
X_{SDT} = Leakage Reactance of step down Transformer
X_{ls}, X'_{lr} = Leakage reactance of the stator and rotor windings
X_M = Magnetizing reactance of the windings
R_S, R'_r = Resistance of stator and rotor windings
H_M, D = Inertia and damping coefficients
J_M = Inertia of rotor
ω_b, ω_d = Base electrical angular velocity, reference frame speed
ω_{rm} = Rotor angular velocity
ψ_{qsm}, ψ_{dsm} = Flux linkages of stator along q-d axes
ψ_{qrm}, ψ_{drm} = Flux linkages of Armature along q-d axes
V_{qsm}, V_{dsm} = Stator voltages in q-d axes
V'_{qsm}, V'_{dsm} = Armature voltages in q-d axes
P_m = Number of poles
P_B = Base rated power
T_{em}, T_{LM} = Electromagnetic torque, Load torque
i_{qsm}, i_{dsm} = Stator currents along q-d axes
i_{Lq}, i_{Ld} = Quadrate and direct axes components of inductance branch of SVC current
i_{Cq}, i_{Cd} = Quadrate and direct axes components of capacitance branch of SVC current
i_{Loq}, i_{Lod} = Quadrate and direct axes components of STATCOM current I_{Lo}
$V_{q\infty}$, $V_{d\infty}$ = Infinite bus voltage along q-d axes
V_M = STATCOM bus voltage

APPENDIX B

Parameters of Drive system and Induction motor for comparing SVC and VSI: $V_{line-line}$ = 575 v, 200 Hp, f = 60 Hz, Rs = 0.011 (p.u), R'r = 0.006(p.u), Xls = 0.0048 (p.u), X'lr = 0.00483 (pu), XM = 2.424 (p.u), J = 2.6 (kg.m^ 2), P = 4

Parameters of induction motor for comparing SVC and STATCOM:
$V_{line-line}$ = 2300 v, 2250 Hp, f = 60 Hz,
Rs = 0.00919 (p.u), R'r = 0.00697 (p.u),
Xls = . 0.0716 (p.u), X'lr = 0.0716 (p.u), XM = 4.13 (p.u),
J = 63.87 (kg.m^2), P = 4

Parameters of transmission line: x_L = 0.04 (p.u), R_L = 0

Parameters of SVC and STATCOM: Xc = 0.5 (p.u), Xin = 0.335 (p.u), C = 1, x_{SDT} = 0.025(p.u), V_{DC0} = 1,

Parameters of PI controller: K_P = 50, K_I = 0.00145, T_W = 0.008.

REFERENCES

Bollen, M.H.J., 2000. Understanding Power Quality Problems: Voltage Sags and Interruptions. 1 Edn., IEEE Press, New York, ISBN: 0-7803-4713-7.

Dugan, R.C., M.F. McGranaghan and H.W. Betty, 1996. Electrical Power Systems Quality. McGraw Hill Companies, London, ISBN: 0-07-018031-8.

Gomez, J.C., M.M. Morcos, C.A. Reineri and G.N. Campatelli, 2002. Behavior of induction motor due to voltage sags and short interruptions. IEEE Trans. Power Delivery, 17: 434-440.

Guasch, L., F. Corcoles and J. Pedra, 2004. Effects of symmetrical and unsymmetrical voltage sags on induction machines. IEEE Trans. Power Delivery, 19: 774-782.

Hedayati, M., 2002. Variable Structure Control (VSC) of flexible ac transmission systems (FACTS) for improving dynamic behavior of induction motors. Proceeding of 3rd Mediterranean Conference and Exhibition on Power Generation, Transmission, Distribution and Energy Conversion, Athens, Greece.

Hedayati, M. and H. Oraee, 2005. Assesment study of shunt FACTS devices for improving dynamic behavior of induction motors. Proc. IEEE Conf. Power Electronics Drives Syst., 2: 1352-1355.

Hingorani, N.G. and L. Gyugyi, 2000. Understanding FACTS: Concepts and Technology of Flexible AC Transmission Systems. IEEE Press, New York, pp: 432.

Juarez, E., A. Hernandez and G. Olguin, 2009. An approach based on analytical expressions to optimal location of voltage sags monitors. IEEE Trans. Power Delivery, 24: 2034-2042.

Rahim, A. and M.F. Kandlawala, 2004. Robust STATCOM voltage controller design using loop shaping technique. Electric Power Syst. Res., 68: 61-74.

Rahim, A. and M. Baber-Abbas, 2007. Self tunning adaptive pole shift STATCOM control for single and multi machine power system. ICGST-ACSE, 7: 55-62.

Seyed, F., A. Rahim and J.M. Ba-Khashwain, 2005. Robust STATCOM controller dsign using PSO based automatic loop shaping procedure. Proceeding of IEEE Conference on Control Applications, August 2005, Toronto, Canada, pp: 440-445.

Song, Y.H. and A.T. Johns, 1999. Flexible AC Transmission Systems. IEE Press, London, ISBN: 0852967713.

Souto, O.C.N., J.C. de Oliveira, P.F. Ribeiro and L.M. Neto, 1998. Power quality impact on performance and associated costs of three-phase induction motors. Proceedings of the 8th International Conference on Harmonics and Quality of Power, Oct. 14-18, IEEE Xplore Press, Athens, Greece, pp: 791-797.

Wang, H.F., 1999. Phillips-heffron model of power systems installed with STATCOM and applications. Proc. IEE Generation Transmission Distribution, 146: 521-527.